Journal of Materials Chemistry A

Accepted Manuscript

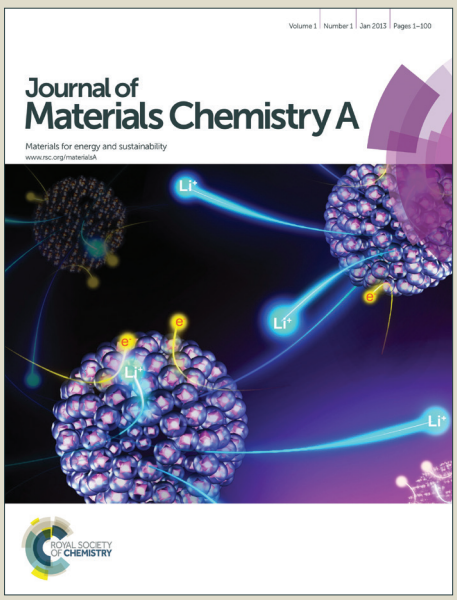

ROYAL SOCIETY OF CHEMISTRY

www.rsc.org/materialsA

Journal Name

RSCPublishing

ARTICLE

From Biomolecule to $Na_3V_2(PO_4)_3$/Nitrogen-Decorated Carbon Hybrids: Highly Reversible Cathodes for Sodium-ion Batteries

Cite this: DOI: 10.1039/xoxxoooooox

Received ooth January 2012,
Accepted ooth January 2012

DOI: 10.1039/xoxxoooooox

www.rsc.org/

Ping Nie, Yaoyao Zhu, Laifa Shen, Gang Pang, Guiyin Xu, Shengyang Dong, Hui Dou and Xiaogang Zhang*

Sodium ion batteries (SIBs) working at room temperature offer promising opportunities for renewable energy storage applications due to the abundant supply and low cost of sodium, yet low capacity, inferior rate capability and limited cycle life remain a significant challenge in their electrochemical operations. Herein, we report the preparation of hierarchically $Na_3V_2(PO_4)_3$/nitrogen-decorated carbon hybrids *via* solvothermal reaction by using biomolecule of adenosine 5'-triphosphate disodium salt (ATP), as a novel precursor and environmentally friendly multifunctional source, including sodium, phosphorus, carbon, nitrogen, simultaneously. The results demonstrate that $Na_3V_2(PO_4)_3$ nanocrystals are encapsulated in interconnected carbon nanosheets with moderate nitrogen doping (2.88 %) to form a bundle-like structure, where the carbon nanosheets not only serve as a highly conducting pathway facilitating electron and ion transport, but a shielding matrix to accommodate volume changes upon electrochemical cycling, thus improving stability and reversibility of the $Na_3V_2(PO_4)_3$ cathode. The obtained materials thus deliver a high reversible capacity of 110.9 mAh g^{-1} at low current rate of 0.2C as well as outstanding rate performance, suggesting that the $Na_3V_2(PO_4)_3$/nitrogen-doped carbon hybrids are promising cathode materials for use in high-performance sodium ion batteries.

Introduction

Energy is most conveniently stored in fossil fuels in the form of chemical energy. The combustion of fossil fuels will pollute the environment and is responsible for changing climate situation. With the increasing environmental concerns and energy shortages, development of clean and renewable energy derived from wind and solar energy has been one of the most significant scientific and engineering duties recently.[1-4] Thus, electric energy storage (EES) is of significance for modern society.[5-8] Among various promising energy storage systems, electrochemical secondary battery technology has been considered to be the best choice for this application due to its flexibility, high energy efficiency, rapid response, and simple maintenance. In particular, Lithium ion batteries (LIBs) have attracted extensive attention for applications ranging from portable electronics to electric vehicles or other energy storage because they can provide much higher energy density compared to other rechargeable battery systems.[9-12] However, the availability of LIBs has been questioned due to the ever increasing demand and limited lithium reserves in the Earth's crust. Based on the data from the US Geological Survey and Meridian International Research, the existing lithium resources could be sustained for *ca.* 65 years from now considering an average growth of 5% per year (total world lithium consumption in 2008: *ca.*21, 280 tons).[13, 14] Accordingly, the new generation of EES systems with low cost and long life is extremely required.

In the word of "*Post Lithium-ion*", sodium ion batteries have been taken into consideration as ideal alternatives to LIBs because of the abundance and ubiquitous distribution of sodium, safety, no toxicity as well as the ability to use electrolytes at lower decomposition potentials and aluminum current collector for anodes.[15-19] Recently, there are an increasing volume of reports on possible materials in both cathodes and anodes for Na-ion batteries, also studies on the stability of various electrolytes.[20, 21] Unfortunately, a drawback for the sodium-ion battery is the relatively large ionic radius of sodium (about 55% larger than that of lithium), resulting in insufficient electrochemical properties, including low reversible capacity, poor cycle stability and inferior rate performance.[22-24] Therefore, a great deal of efforts should been made to develop suitable host structures with sufficiently large interstitial space to accommodate Na ions and enable reversible and rapid ion insertion and extraction.[25-28] $Na_3V_2(PO_4)_3$ with NASICON structure is a good cathode material that has received considerable attention for Na-ion batteries due to its high theoretical energy density (~400 Wh kg^{-1}, 117.6 mAh g^{-1}×3.4 V), good thermal stability (450 ℃), open 3D framework with large interstitial channels.[29-33] Moreover, this material has two different voltage plateaus at around 3.4 V and 1.6 V, corresponding to the V^{3+}/V^{4+} and V^{3+}/V^{2+} redox couples, respectively. The unique double potentials property makes it a

perfect candidate for used as an anode and a cathode in symmetric batteries, simultaneously.[34] However, one obstacle delaying the commercialization of $Na_3V_2(PO_4)_3$ is the poor electronic conductivity, which leads to low Coulombic efficiency and poor cycle performance. More recently, research and development efforts to address the issues are focused on the improvement of the conductivity, reduction in grain size, and prevention of the particle aggregation. As a result, high specific capacities in terms of ultrafast rate performance have been achieved by many research groups.[35, 36] Despite continuous progress made in recent years, only a few reports of $Na_3V_2(PO_4)_3$ as electrodes for sodium ion batteries exist in the literature. Developing a facile and reliable synthesis procedure for producing high-rate and long-life $Na_3V_2(PO_4)_3$ with well-defined architectures is highly desirable and still remains a challenge.

Currently, naturally biological materials which are abundant, renewable, and eco-friendly, have been widely utilized as new raw materials for functional materials with novel morphologies and properties.[37, 38] For example, Su *et al.*[39] fabricated $LiFePO_4$ nano/microspheres by using phytic acid as a biomass precursor, which showed excellent performance for lithium ion batteries. Mitlin *et al.*[40] reported the hydrothermal-based synthesis of two-dimensional and interconnected carbon nanosheets from hemp bast fiber with superior electrochemical capacitance properties. The resultant nanosheets electrodes can work even down to 0 ℃ and display some of the best power-energy combinations reported in the literature for any carbon material, also the peat moss-derived carbon nanosheets anode for sodium ion battery.[41] Activated carbons derived from coconut shells also exhibits favorable energy density and extraordinary cyclability when used as cathode materials for Li-ion capacitors.[42] Wang and co-workers[43] investigated a hierarchical porous carbon obtained from fish scales for lithium sulfur batteries. The resultant electrode displayed superb electrochemical performance in numerous respects, including high reversible capacity, rate capability, and cycling stability. These amazing achievements light the way to using renewable biomolecules as precursors for the preparation of electrode materials for sodium ion battery application.

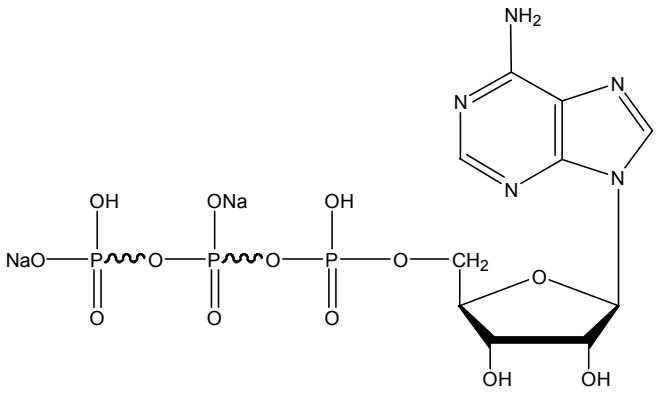

Fig. 1 Chemical structure of adenosine 5'-triphosphate disodium salt.

In this paper, a facile template-free solvothermal method has been developed for the first time to fabricate bundle-like $Na_3V_2(PO_4)_3$ /nitrogen-doped carbon nanoarchitectures by using adenosine 5'-triphosphate disodium salt, the most common energy carrier of the cell in biological systems,[44] as novel and green phosphorus, carbon, nitrogen and sodium sources, simultaneously. $Na_3V_2(PO_4)_3$ nanocrystals were encapsulated in thin carbon nanosheets with nitrogen doping to form a bundle-like composite, in which the carbon nanosheets not only serve as a highly conducting pathway facilitating electron and ion transport, but a shielding matrix to accommodate volume changes upon electrochemical cycling, thus improving stability and reversibility of the $Na_3V_2(PO_4)_3$ cathode. Consequently, the hybrid exhibits a high specific capacity of 110.9 mAh g^{-1} at a 0.2C rate, and a remarkable cyclability, suggesting a potential application as a new cathode for sodium ion batteries.

Results and discussion

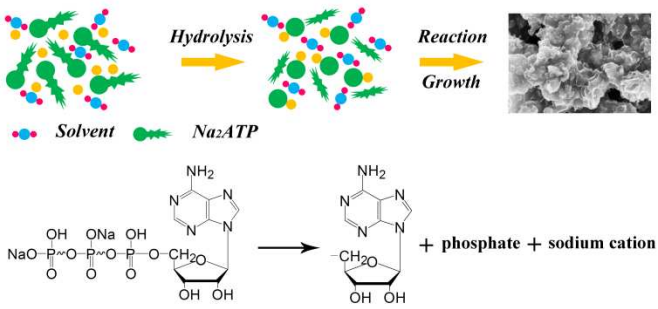

Scheme 1 Schematic illustration of the synthetic process of $Na_3V_2(PO_4)_3$/nitrogen-doped carbon nanosheet composites and decomposition reaction of adenosine 5'-triphosphate disodium salt under solvothermal environment.

Adenosine triphosphate, the most abundant ribonucleotide within cells, is not only one of the most widely existing biomolecules in nature but also transports chemical energy as the "molecular unit of currency" of the cell and various cellular processes.[45-47] ATP plays an important role in cell signaling and cellular reaction. It also involves in the process of DNA replication, transcription, and other basic activities of life.[48-50] As shown in Fig. 1, there are high-energy phosphorus bonds and an ordered carbon compound backbone in the structure of ATP. Upon hydrolysis reaction, PO_4^{3-}, Na ions, nitrogen-containing precursors and a large amount of free energy could be released, which make it excellent natural sources for the synthesis of various inorganic nanoparticles.[51, 52] Moreover, ATP biomolecules can also act as a stabilizer and nucleating agent during the synthesis. Compared with the commonly used inorganic phosphorus sources, ATP biomolecules have several significant advantages. Firstly, phosphorus exists in the form of phosphate groups. ATP biomolecules hydrolyze to produce PO_4^{3-} ions and other molecules in a controlled manner under certain conditions, which could avoid the fast nucleation and disordered growth of nanoparticles. Secondly, the morphology, size, and structure of the products are usually influenced by its preparation process. Therefore, it is very significant to prepare materials using natural molecules as the structure control agent. Moreover, ATP is abundant in nature, low cost and environmentally friendly, thus endowing them great application potential for various phosphate-based materials.

The schematic illustration shown in Scheme 1 demonstrates the fabrication process of bundle-like $Na_3V_2(PO_4)_3$/nitrogen-doped carbon nanocomposites. Firstly, ATP molecules hydrolyze to produce PO_4^{3-}, Na cation, and adenosine molecule in mixed solvents of deionized water and polyethylene glycol under solvothermal conditions. In the subsequent process, these molecules react with vanadium ions to form $Na_3V_2(PO_4)_3$ intermediate phases, and adenosine molecule acts as a stabilizer and biocarbon source for nitrogen-containing precursors. After

a complicated dissolution-recrystallization process, bundle-like $Na_3V_2(PO_4)_3$/C hybrids are obtained followed by annealing under nitrogen atmosphere.

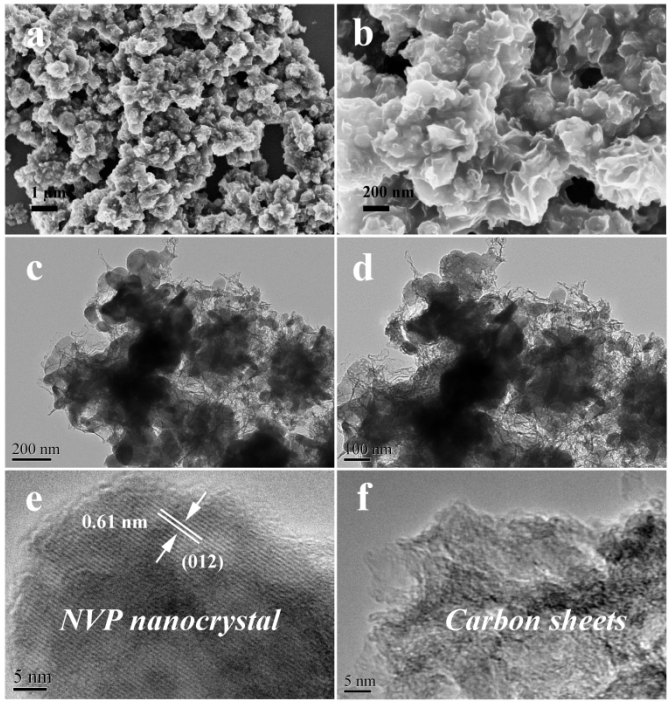

Fig. 2 (a, b) FESEM and (c-f) TEM images of the as-synthesized bundle-like $Na_3V_2(PO_4)_3$/C nanostructures.

The size and morphology of the as-synthesized $Na_3V_2(PO_4)_3$ were investigated by field-emission scanning electron microscopy (FESEM) and transmission electron microscope (TEM). As shown in Fig. 2a, b, the $Na_3V_2(PO_4)_3$/C compositesconsist of a bunble-like shape with the particle size of 500-800 nm. SEM image at higher magnification (Fig. 2b) reveals the highly interconnected sheet-like structure of the samples, and the nanosheets are interconnected and overlap to form a 3D porous structure. TEM images (Fig. 2c, d) further highlight the structure of $Na_3V_2(PO_4)_3$, one can interestingly find that the product consists of highly interconnected nanosheets and nanocrytals with sizes of a few tens of nanometers. The high resolution transmission electron microscopy (HRTEM) image of a selected nanoparticles in Fig. 2e clearly demonstrate the phase of $Na_3V_2(PO_4)_3$, where the clear lattice fringes with spacing of 6.1 Å, corresponding to the (012) plane of rhombohedral $Na_3V_2(PO_4)_3$.[29] Furthermore, the amorphous state of the nanosheets indicates the components of carbon (Fig. 2f). The energy dispersive X-ray spectra (EDS) elemental mappings (Fig. S1) illustrate a homogeneous element distribution (Na, O, V, P, and C species) with a small amount of nitrogen in the composites. No other impurity elements were detected. Moreover, the distributions of these chemical elements were in the range of the EDS mapping of C, revealing the formation of targeted structure. Hence, the adenosine molecules have been transformed into nitrogen containing carbon after pyrolysis. The first-principles calculations and experimental studies demonstrate that the doping by N could render materials enhanced electrical conductivity and electrochemical reactivity.[53-55] For comparison, when $NH_4H_2PO_4$ was used as the phosphorus source under the same conditions, the control samples consist of agglomerated nanoparticles, as shown in Fig. S2. The results indicate that the biomolecules act as both a precursor for nitrogen, phosphorus, carbon, sodium source and a bio-template, which has a great effect on the morphology regulation and crystal growth during solvothermal process. In summary, nano-sized $Na_3V_2(PO_4)_3$ particles are modified by adenosine-derived nitrogen doped carbon nanosheets to form bundle-like hierarchical structures.

The crystal structure and phase purity of the resulting $Na_3V_2(PO_4)_3$/C samples were investigated by X-ray diffraction (XRD). Fig. S3 shows the XRD patterns of the two representative samples prepared by using ATP and $NH_4H_2PO_4$ as the phosphorus sources, respectively. All diffraction peaks are well in accordance with the NASICON structure with *R-3c* space group (rhombohedral unit cell, No.167).[31] A Rietveld refinement analysis (Fig. 3b) was performed to estimate the bundle-like $Na_3V_2(PO_4)_3$ phase more precisely. As summarized in Table 1, the cell parameters obtained by Rietveld refinement were a= 8.734 (1) Å, c = 21.822 (2) Å and V = 1441.8 (2) Å^3, which correspond well with the existing values in literature and JCPDS card No.53-0018.[30, 31] Fig. 3a represents the schematic illustration of the NASICON type structure, which is built on a $[V_2(PO_4)_3]$ unit of VO_6 octahedra sharing all the corners with PO_4 tetrahedra, where two octahedral VO_6 connected with three tetrahedral PO_4 constitute a basic unit. The two independent sodium atoms are located in the voids/channels of the framework with two different oxygen environments, one Na^+ occupies the 6b site (Na1) and the other one is located in 18e site (Na2).[29, 31] This open 3D framework offers large interstitial spaces for Na^+ accommodation, also channels allowing rapid transport of sodium ions and electron throughout the lattice.

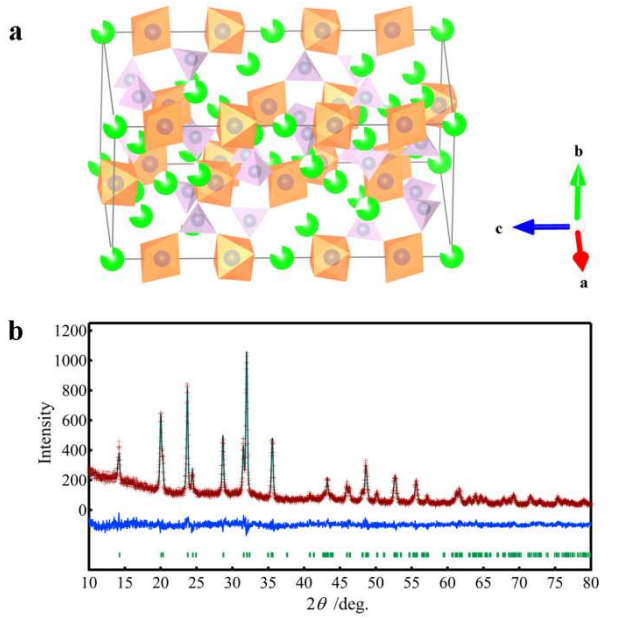

Fig. 3 (a) Schematic representation of the crystal structure of $Na_3V_2(PO_4)_3$, (b) Rietveld refinement of the observed XRD pattern for $Na_3V_2(PO_4)_3$/C samples synthesis from ATP.

X-ray photoelectron spectroscopy (XPS) was employed to further characterized the bundle-like $Na_3V_2(PO_4)_3$/N-doped carbon composite. The survey XPS spectrum of the material reveals the presence of Na, V, P, C, and N elements, indicating the successful incorporation of nitrogen, consistent with the EDS analysis mentioned above (Fig. 4a). To clarify the effect

of N-doping, we analyzed the high-resolution N 1s peak of the hybrid (Fig. 4b). The N1s spectrum could be deconvoluted into four peaks centered at 398.5, 400.9, 402.5 and 406.4 eV, assigned to pyridinic N, pyrrolic N, graphitic N and oxygenated N, respectively.[56, 57] The total N content is calculated to be 2.88 atomic%. It has been widely established that the pyridinic-N species cause structural deformation and expose planar edges or defect sites in carbon materials, while pyrrolic N and graphitic-N will enable the surface adsorption and higher electronic conductivity of the carbon, respectively. Thus, nitrogen-doped carbon would be electrochemically more active. Compared with the post synthesized modification, our work opens new perspectives to develop functional materials with nitrogen doping for new energy storage systems.

Table 1 Atomic coordinates, isotropic thermal parameters and occupation numbers for $Na_3V_2(PO_4)_3$ phase refined from X-ray powder diffraction data. NASICON-type structure in space group R-3c (No. 167); cell parameters: a = 8.734 (1) Å, c = 21.822 (2) Å, V = 1441.8 (2) Å^3 and Z = 6; R_{wp} = 11.58 %, R_p = 8.82 %, R_I = 8.826 %, S = 1.47.

Atom	Site	g	x	y	Z	B (Å^2)
Na	6b	1	0	0	0	1.1
Na	18e	1	0.641	0	1/4	1.5
V	12c	1	0	0	0.149	1.6
P	18e	1	0.287	0	1/4	0.8
O1	36f	1	0.178	0.967	0.192	0.82
O2	36f	1	0.192	0.166	0.089	0.9

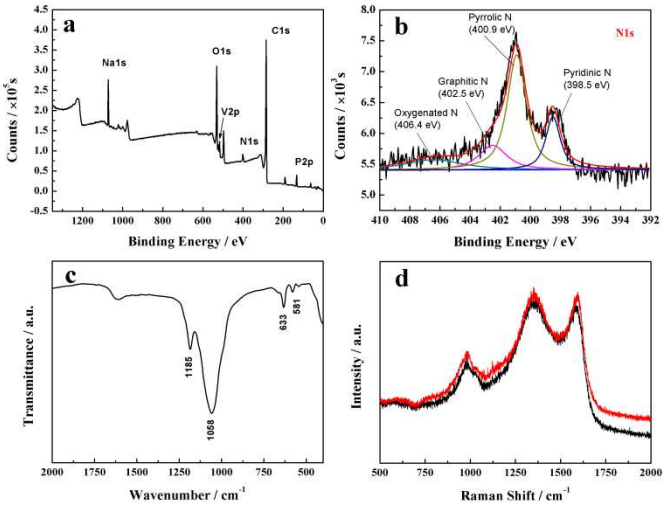

Fig. 4 (a) Survey XPS spectrum, (b) N 1s XPS spectrum, (c) FTIR spectrum of bundle-like $Na_3V_2(PO_4)_3$/C nanostructures, and (d) Raman spectra of $Na_3V_2(PO_4)_3$/C samples prepared by using ATP (black curve) and $NH_4H_2PO_4$ (red curve) as the phosphorus sources.

The compositions of the as-prepared material were also identified by Fourier transform infrared (FT-IR) spectroscopy as shown in Fig. 4c. The bands at 581 and 1058 cm^{-1} suggest the presence of P-O bonds in PO_4 tetrahedra, and the vibration from V^{3+}-O^{2-} bonds in isolated VO_6 octahedra is located at 633 cm^{-1}. In addition, the IR bands in the range of 1150-1250 cm^{-1} can be ascribed to the stretching vibration of terminal PO_4 units, in agreement with the assignments previously reported in the literature.[58] Raman spectroscopy studies were carried out to investigate the structure features of the resulting $Na_3V_2(PO_4)_3$/C composites. Fig. 4d displays the Raman spectra of the carbon coated $Na_3V_2(PO_4)_3$ and the nitrogen doped modified one. The peaks at 1350 cm^{-1} (D band) and 1595 cm^{-1} (G-band) can be seen clearly in both samples, suggesting the existence of carbon in the materials, which corresponds to the lattice defects, edges and disorder in the C-C system (sp^3 hybridization) and the C-C stretching mode of highly ordered graphitic carbon (sp^2 hybridization), respectively. Meanwhile, the $Na_3V_2(PO_4)_3$ exhibits characteristic peak located at 984 cm^{-1}.[30, 59] The Brunauer-Emmet-Teller (BET) specific surface area of $Na_3V_2(PO_4)_3$/nitrogen-doped carbon hybrid was further investigated by N_2 adsorption-desorption isotherm. As shown in Fig. S4, the composites possessed a relatively high specific surface area of 83.6 m^2 g^{-1}, and the pore volume was~0.279 cm^3 g^{-1}. The carbon content is estimated to be 20.25 wt% and 5.40 wt% in bundle-like $Na_3V_2(PO_4)_3$ and the comparative one, respectively, as measured by thermogravimetric (TG) analysis in an air atmosphere (Fig. S5). The high carbon content in the former is closely related to the carbon compound backbone in the structure of ATP molecule.

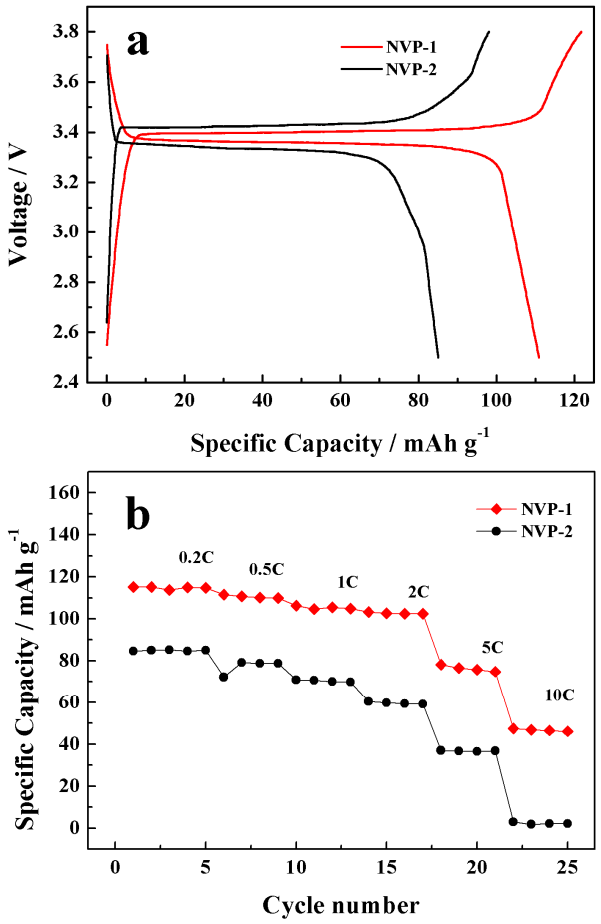

Fig. 5 (a) Galvanostatic charge/discharge curves for the $Na_3V_2(PO_4)_3$ cells at a rate of 0.2C in the voltage range of 2.5 and 3.8 V, (b) Cycling performance of the two samples at various current densities.

Intrigued by the structural features of the obtained composites, electrochemical measurements of the $Na_3V_2(PO_4)_3$ electrodes were performed in 2032 coin-type cells at the room temperature. Fig. 5a shows galvanostatic charge/discharge profiles of the $Na_3V_2(PO_4)_3$ electrodes in the potential window of 2.5-3.8 V *vs.* Na^+/Na at a rate of 0.2 C (1C = 117.6 mAh g^{-1}). The bundle-like $Na_3V_2(PO_4)_3$/C hybrids afford initial charge

and discharge capacities of 121.7 and 110.9 mAh g^{-1}, yielding an efficiency of 91.1%. The irreversible capacity loss may mainly stem from kinetic limitations by structural changes during sodium de/insertion.[59] The distinct voltage plateaus demonstrate a two-phase reaction between $Na_3V_2(PO_4)_3/NaV_2(PO_4)_3$, corresponding to the V^{4+}/V^{3+} redox couple, where the electrochemical Na^+ insertion/extraction processes occurring at $Na_3V_2(PO_4)_3$ electrode can be expressed by *Equation (1)*:

$$Na_3V_2(PO_4)_3 \leftrightarrow NaV_2(PO_4)_3 + 2Na^+ + 2e^- \quad (1)$$

resembling the results in previous reports.[59] In contrast, the nitrogen free $Na_3V_2(PO_4)_3$/C nanocomposites delivered a discharge capacity of 85 mAh g^{-1}. Interestingly, an obvious narrow gap between charge and discharge voltage profiles is observed for the bundle-like $Na_3V_2(PO_4)_3$ and the sample presents a higher Coulombic efficiency than the $Na_3V_2(PO_4)_3$ nanoparticles (86.7%). It is noted that the enhanced performances of bundle-like $Na_3V_2(PO_4)_3$/C material may originate from highly conductive network represented by the interparticular nitrogen-doping carbon nanosheets located between $Na_3V_2(PO_4)_3$ nanocrystals.

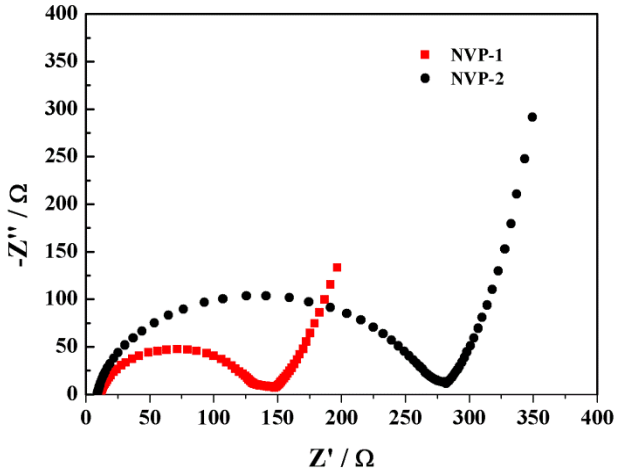

Fig. 6 Nyquist impedance plots of the $Na_3V_2(PO_4)_3$ electrodes measured before cycling.

The charge/discharge rate performance of the $Na_3V_2(PO_4)_3$/C composite was investigated by cycling at various current densities. An extraordinary high-rate capability is demonstrated in Fig. 5b in which the cell delivers a high reversible capacity of 110.7, 104.7, 102.6, 76.6 mAh g^{-1} at current rates of 0.5C, 1C, 2C and 5C, respectively. Even when the C-rate was increased to 10C, a remarkably reversible and stable capacity of 46.8 mAh g^{-1} was still preserved. This corresponds to a charge or discharge time of 6 minutes, indicating the excellent rate capability of the cathode. It is worth noting that the as-prepared bundle-like $Na_3V_2(PO_4)_3$ material demonstrates much better performance compared to the bare $Na_3V_2(PO_4)_3$ without N-doping carbon nanosheets modification, indicating the positive effect of the unique structure. Overall, the sodium storage properties of bundle-like $Na_3V_2(PO_4)_3$/carbon nanosheets hybrids in terms of specific capacity and rate performance are comparable or even superior to the reported $Na_3V_2(PO_4)_3$ cathode materials in the literature,[29, 35, 58] which renders the nanocomposite highly desirable for applications in large-scale electric energy storage and electric vehicles.

To further establish the relationship between electrochemical performance and electrode kinetics for both $Na_3V_2(PO_4)_3$ cathodes, impedance Nyquist plots was collected on fresh cells (Fig. 6). The impedance spectra of both electrodes consist of a single depressed semicircle in the high frequency region and an inclined line at low frequency, corresponding to the charge-transfer resistance (R_{ct}) and the solid-state diffusion of ions in the active materials, respectively. The bundle-like $Na_3V_2(PO_4)_3$ electrodes show smaller diameter of semicircles in the Nyquist plots than those of the corresponding bare $Na_3V_2(PO_4)_3$ without N-doping carbon nanosheets, indicating lower R_{ct} and better kinetics for sodium ion insertion reactions. This result clearly implies that the electronic conductivity of $Na_3V_2(PO_4)_3$ has been remarkably improved by coupling N-doping carbon nanosheets.

In the light of the results, the superior performance of the $Na_3V_2(PO_4)_3$/carbon nanosheets composite could be ascribed to its unique nanoarchitecture and favorable morphology. Firstly, the porous 3D structure and open channels between $Na_3V_2(PO_4)_3$ nanocrystals and carbon nanosheets offer favorable paths for electrolyte penetration, facilitating fast charge transfer across the electrolyte/electrode interface.[60] Secondly, the nitrogen doping in the carbon matrix can introduce a lot of surface defects and enhance the electrochemical reactivity. Furthermore, the well-crystallized nature and nanoscale effect of the $Na_3V_2(PO_4)_3$ nanocrystals provide relatively shorter Na^+ diffusion pathways, thus facilitating the fast kinetics of electrochemical reactions.[61, 62] Lastly, the $Na_3V_2(PO_4)_3$ nanocrystals are encapsulated in the large-area carbon nanosheets multiplexed networks, which further strengthen the structural integrity of the hybrids, prevent the aggregation and volume change during Na insertion and extraction, aslo enable reasonable electronic conductivity of the $Na_3V_2(PO_4)_3$ material. All in all, the above synergetic effect favors the high reversible capacity as well as superior rate performance of the bundle-like $Na_3V_2(PO_4)_3$/nitrogen-doped carbon nanocomposite.

Conclusions

In summary, bundle-like $Na_3V_2(PO_4)_3$/nitrogen-doped carbon composite has been synthesized *via* solvothermal reaction by using a high-energy biomolecule for the first time. In the system, ATP biomolecule acts as a multifunctional source, including sodium, phosphorus, carbon, nitrogen, also a biotemplate to control the formation of the hierarchical structure. The unique porous 3D structure offer favorable paths for electrolyte penetration and mass/charge transfer, and the newly found nitrogen-doped carbon nanosheets enable high electronic conductivity of the $Na_3V_2(PO_4)_3$, thus facilitating the fast kinetics of electrochemical reactions. These features combined with the nanoscale effect of the $Na_3V_2(PO_4)_3$ nanocrystals, the as-fabricated hybrids exhibit extremely high sodium storage capacities and impressive rate capability when used as cathode materials. Our design for the synthesis of $Na_3V_2(PO_4)_3$ by using ATP as precursors represents a promising direction and new prospect towards developing novel types of functional materials for energy storage devices.

Acknowledgements

This work is financially supported by the National Program on Key Basic Research Project of China (973 Program, No. 2014CB239701), National Natural Science Foundation of China (No. 21173120, 21103091, 51372116), Natural Science Foundation of Jiangsu Province (No.BK2011030), and Fundamental Research Funds for the Central Universities of

NUAA (NP2014403). P. Nie and Y. Zhu also would like to thank the Funding for Outstanding Doctoral Dissertation in NUAA (No.BCXJ14-12), the Founding of Graduate Innovation Center in NUAA (No. kfjj201438) and Funding of Jiangsu Innovation Program for Graduate Education (No.KYLX_0254) and the Fundamental Research Funds for the Central Universities.

Notes and references

College of Material Science and Engineering, Key Laboratory for Intelligent Nano Materials and Devices of Ministry of Education, Nanjing University of Aeronautics and Astronautics, Nanjing, China. Fax: +86 025 52112626; Tel: +86 025 52112918; E-mail: azhangxg@163.com

Electronic Supplementary Information (ESI) available: [Detailed experimental procedures and supplementary Figures]. See DOI: 10.1039/b000000x/

1. P. Hartmann, C. L. Bender, M. Vračar, A. K. Dürr, A. Garsuch, J. Janek and P. Adelhelm, *Nat. Mater.*, 2013, 12, 228-232.
2. J. B. Goodenough, *Energy Environ. Sci.*, 2014, 7, 14-18.
3. B. Dunn, H. Kamath and J.-M. Tarascon, *Science*, 2011, 334, 928-935.
4. C. Yuan, H. B. Wu, Y. Xie and X. W. Lou, *Angew. Chem. Int. Ed.*, 2014, 53, 1488-1504.
5. C. D. Wessells, R. A. Huggins and Y. Cui, *Nat. Commun.*, 2011, 2, 550.
6. M. Pasta, C. D. Wessells, R. A. Huggins and Y. Cui, *Nat. Commun.*, 2012, 3, 1149.
7. M. Pasta, C. D. Wessells, N. Liu, J. Nelson, M. T. McDowell, R. A. Huggins, M. F. Toney and Y. Cui, *Nat. Commun.*, 2014, 5.
8. H. Pang, C. Wei, Y. Ma, S. Zhao, G. Li, J. Zhang, J. Chen and S. Li, *ChemPlusChem*, 2013, 78, 546-553.
9. N.-S. Choi, Z. Chen, S. A. Freunberger, X. Ji, Y.-K. Sun, K. Amine, G. Yushin, L. F. Nazar, J. Cho and P. G. Bruce, *Angew. Chem. Int. Ed.*, 2012, 51, 9994-10024.
10. J. M. Tarascon and M. Armand, *Nature*, 2001, 414, 359-367.
11. P. Nie, L. Shen, F. Zhang, L. Chen, H. Deng and X. Zhang, *CrystEngComm*, 2012, 14, 4284-4288.
12. J. Popovic, R. Demir-Cakan, J. Tornow, M. Morcrette, D. S. Su, R. Schlögl, M. Antonietti and M.-M. Titirici, *Small*, 2011, 7, 1127-1135.
13. C.-X. Zu and H. Li, *Energy Environ. Sci.*, 2011, 4, 2614-2624.
14. H. Pan, Y.-S. Hu and L. Chen, *Energy Environ. Sci.*, 2013, 6, 2338-2360.
15. C. Delmas, J.-J. Braconnier, C. Fouassier and P. Hagenmuller, *Solid State Ionics*, 1981, 3–4, 165-169.
16. V. Raju, J. Rains, C. Gates, W. Luo, X. Wang, W. F. Stickle, G. D. Stucky and X. Ji, *Nano Lett.*, 2014, 14, 4119-4124.
17. N. Yabuuchi, M. Kajiyama, J. Iwatate, H. Nishikawa, S. Hitomi, R. Okuyama, R. Usui, Y. Yamada and S. Komaba, *Nat. Mater.*, 2012, 11, 512-517.
18. R. Berthelot, D. Carlier and C. Delmas, *Nat. Mater.*, 2011, 10, 74-80.
19. H. Yu, S. Guo, Y. Zhu, M. Ishida and H. Zhou, *Chem. Commun.*, 2014, 50, 457-459.
20. C. Luo, Y. Zhu, Y. Xu, Y. Liu, T. Gao, J. Wang and C. Wang, *J. Power Sources*, 2014, 250, 372-378.
21. A. Bhide, J. Hofmann, A. Katharina Durr, J. Janek and P. Adelhelm, *Phys. Chem. Chem. Phys.*, 2014, 16, 1987-1998.
22. K. Sakaushi, E. Hosono, G. Nickerl, T. Gemming, H. Zhou, S. Kaskel and J. Eckert, *Nat. Commun.*, 2013, 4, 1485.
23. Y. Wang, X. Yu, S. Xu, J. Bai, R. Xiao, Y.-S. Hu, H. Li, X.-Q. Yang, L. Chen and X. Huang, *Nat. Commun.*, 2013, 4.
24. S. Y. Lim, H. Kim, J. Chung, J. H. Lee, B. G. Kim, J.-J. Choi, K. Y. Chung, W. Cho, S.-J. Kim, W. A. Goddard, Y. Jung and J. W. Choi, *Proc. Natl. Acad. Sci.*, 2014, 111, 599-604.
25. B. Jache and P. Adelhelm, *Angew. Chem. Int. Ed.*, 2014, DOI: 10.1002/anie.201403734.
26. G. Pang, C. Yuan, P. Nie, B. Ding, J. Zhu and X. Zhang, *Nanoscale*, 2014, 6, 6328-6334.
27. P. Nie, L. Shen, H. Luo, B. Ding, G. Xu, J. Wang and X. Zhang, *J. Mater. Chem. A*, 2014, 2, 5852-5857.
28. C. Luo, Y. Xu, Y. Zhu, Y. Liu, S. Zheng, Y. Liu, A. Langrock and C. Wang, *ACS Nano*, 2013, 7, 8003-8010.
29. Z. Jian, L. Zhao, H. Pan, Y.-S. Hu, H. Li, W. Chen and L. Chen, *Electrochem. Commun.*, 2012, 14, 86-89.
30. Z. Jian, W. Han, X. Lu, H. Yang, Y.-S. Hu, J. Zhou, Z. Zhou, J. Li, W. Chen, D. Chen and L. Chen, *Adv. Energy Mater.*, 2013, 3, 156-160.
31. K. Saravanan, C. W. Mason, A. Rudola, K. H. Wong and P. Balaya, *Adv. Energy Mater.*, 2013, 3, 444-450.
32. J. Kang, S. Baek, V. Mathew, J. Gim, J. Song, H. Park, E. Chae, A. K. Rai and J. Kim, *J. Mater. Chem.*, 2012, 22, 20857-20860.
33. W. Shen, C. Wang, H. Liu and W. Yang, *Chem.–Eur. J.*, 2013, 19, 14712-14718.
34. L. S. Plashnitsa, E. Kobayashi, Y. Noguchi, S. Okada and J.-i. Yamaki, *J. Electrochem. Soc.*, 2010, 157, A536-A543.
35. J. Liu, K. Tang, K. Song, P. A. van Aken, Y. Yu and J. Maier, *Nanoscale*, 2014, 6, 5081-5086.
36. C. Zhu, K. Song, P. A. van Aken, J. Maier and Y. Yu, *Nano Lett.*, 2014, 14, 2175-2180.
37. L. Wang, Z. Schnepp and M. M. Titirici, *J. Mater. Chem. A*, 2013, 1, 5269-5273.
38. M.-M. Titirici, M. Antonietti and N. Baccile, *Green Chem.*, 2008, 10, 1204-1212.
39. J. Su, X.-L. Wu, C.-P. Yang, J.-S. Lee, J. Kim and Y.-G. Guo, *J. Phys. Chem. C*, 2012, 116, 5019-5024.
40. H. Wang, Z. Xu, A. Kohandehghan, Z. Li, K. Cui, X. Tan, T. J. Stephenson, C. K. King'ondu, C. M. B. Holt, B. C. Olsen, J. K. Tak, D. Harfield, A. O. Anyia and D. Mitlin, *ACS Nano*, 2013, 7, 5131-5141.
41. J. Ding, H. Wang, Z. Li, A. Kohandehghan, K. Cui, Z. Xu, B. Zahiri, X. Tan, E. M. Lotfabad, B. C. Olsen and D. Mitlin, *ACS Nano*, 2013, 7, 11004-11015.
42. A. Jain, V. Aravindan, S. Jayaraman, P. S. Kumar, R. Balasubramanian, S. Ramakrishna, S. Madhavi and M. P. Srinivasan, *Sci. Rep.*, 2013, 3.
43. S. Zhao, C. Li, W. Wang, H. Zhang, M. Gao, X. Xiong, A. Wang, K. Yuan, Y. Huang and F. Wang, *J. Mater. Chem. A*, 2013, 1, 3334-3339.
44. S. Biswas, K. Kinbara, T. Niwa, H. Taguchi, N. Ishii, S. Watanabe, K. Miyata, K. Kataoka and T. Aida, *Nat. Chem.*, 2013, 5, 613-620.
45. L. Berti and G. A. Burley, *Nat. Nanotech.*, 2008, 3, 81-87.
46. H. Cao, L. Zhang, H. Zheng and Z. Wang, *J. Phys. Chem. C*, 2010, 114, 18352-18357.

47. M.-a. Morikawa, M. Yoshihara, T. Endo and N. Kimizuka, *J. Am. Chem. Soc.*, 2005, 127, 1358-1359.
48. R. Mo, T. Jiang and Z. Gu, *Angew. Chem. Int. Ed.*, 2014, 53, 5815-5820.
49. Y. Guo, X. Sun, G. Yang and J. liu, *Chem. Commun.*, 2014, 50, 7659-7662.
50. R. Mo, T. Jiang, R. DiSanto, W. Tai and Z. Gu, *Nat. Commun.*, 2014, 5.
51. C. Qi, Y.-J. Zhu, X.-Y. Zhao, B.-Q. Lu, Q.-L. Tang, J. Zhao and F. Chen, *Chem.–Eur. J.*, 2013, 19, 981-987.
52. X. Zhang, Z. Bi, W. He, G. Yang, H. Liu and Y. Yue, *Energy Environ. Sci.*, 2014, 7, 2285-2294.
53. C. Wei, Y. Liu, X. Li, J. Zhao, Z. Ren and H. Pang, *ChemElectroChem*, 2014, 1, 799-807.
54. L. Zhao, Y.-S. Hu, H. Li, Z. Wang and L. Chen, *Adv. Mater.*, 2011, 23, 1385-1388.
55. E. Yoo, J. Nakamura and H. Zhou, *Energy Environ. Sci.*, 2012, 5, 6928-6932.
56. H. Li, L. Shen, K. Yin, J. Ji, J. Wang, X. Wang and X. Zhang, *J. Mater. Chem. A*, 2013, 1, 7270-7276.
57. Y. Hou, T. Huang, Z. Wen, S. Mao, S. Cui and J. Chen, *Adv. Energy Mater.*, 2014, DOI: 10.1002/aenm.201400337.
58. S. Y. Lim, H. Kim, R. A. Shakoor, Y. Jung and J. W. Choi, *J. Electrochem. Soc.*, 2012, 159, A1393-A1397.
59. Y. H. Jung, C. H. Lim and D. K. Kim, *J. Mater. Chem. A*, 2013, 1, 11350-11354.
60. H. B. Wu, H. Pang and X. W. Lou, *Energy Environ. Sci.*, 2013, 6, 3619-3626.
61. L. Yu, L. Zhang, H. B. Wu and X. W. Lou, *Angew. Chem. Int. Ed.*, 2014, 53, 3711-3714.
62. W. Luo, S. Lorger, B. Wang, C. Bommier and X. Ji, *Chem. Commun.*, 2014, 50, 5435-5437.

Table of contents entry

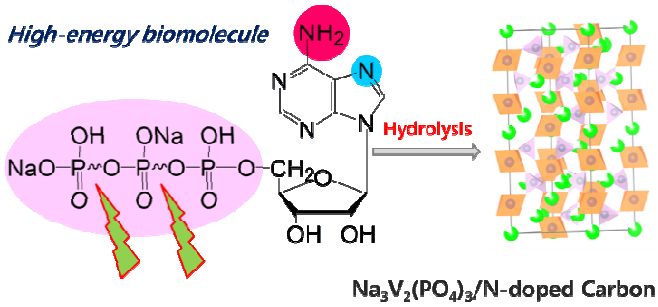

Biomolecule for sodium ion battery: We present important findings related to a high energy biomolecule, adenosine 5'-triphosphate disodium salt (ATP), as a novel precursor and environmentally friendly multifunctional source for the synthesis of bundle-like $Na_3V_2(PO_4)_3$/nitrogen-decorated carbon nanocomposites.